Published as: *Neuron*. 2013 June 19; 78(6): 1024–1035.

Arc/Arg3.1 Is a Postsynaptic Mediator of Activity-Dependent Synapse Elimination in the Developing Cerebellum

Takayasu Mikuni[1], **Naofumi Uesaka**[1], **Hiroyuki Okuno**[2], **Hirokazu Hirai**[3], **Karl Deisseroth**[4], **Haruhiko Bito**[2], and **Masanobu Kano**[1]

[1]Department of Neurophysiology, Graduate School of Medicine, The University of Tokyo, Tokyo 113-0033, Japan

[2]Department of Neurochemistry, Graduate School of Medicine, The University of Tokyo, Tokyo 113-0033, Japan

[3]Department of Neurophysiology, Graduate School of Medicine, Gunma University, Gunma 371-8511, Japan

[4]Departments of Bioengineering, Psychiatry, and Behavioral Sciences, and Howard Hughes Medical Institute, Stanford University, Stanford, CA 94305, USA

SUMMARY

Neural circuits are shaped by activity-dependent elimination of redundant synapses during postnatal development. In many systems, postsynaptic activity is known to be crucial, but the precise mechanisms remain elusive. Here we report that the immediate early gene *Arc/Arg3.1* mediates elimination of surplus climbing fiber (CF) to Purkinje cell (PC) synapses in the developing cerebellum. CF synapse elimination was accelerated when activity of channelrhodopsin-2 expressing PCs was elevated by 2-day photo-stimulation. This acceleration was suppressed by PC-specific knockdown of either P/Q-type voltage-dependent Ca^{2+} channel (VDCC) or Arc. PC-specific Arc knockdown had no appreciable effect until around postnatal day 11, but significantly impaired CF synapse elimination thereafter, leaving redundant CF terminals on PC somata. The effect of Arc knockdown was occluded by simultaneous knockdown of P/Q-type VDCC in PCs. We conclude that Arc mediates the final stage of CF synapse elimination downstream of P/Q-type VDCC by removing CF synapses from PC somata.

INTRODUCTION

How neural circuits are shaped during postnatal development is a fundamental issue in neuroscience. Formation of neural circuits in many regions of the nervous system is initiated by exuberant synaptogenesis around birth. Necessary synapses are then selectively strengthened whereas redundant connections are weakened and eventually eliminated during the course of postnatal development (Arsenault and Zhang, 2006; Chen and Regehr, 2000; Kano and Hashimoto, 2009; Lu and Trussell, 2007; Purves and Lichtman, 1980). This process is known as synapse elimination, and is widely thought to be crucial for shaping mature neural circuits depending on neural activity (Buffelli et al., 2003; Hensch, 2004;

Correspondence: Masanobu Kano, Department of Neurophysiology, Graduate School of Medicine, The University of Tokyo, 7-3-1 Hongo, Bunkyo-ku, Tokyo 113-0033, Japan, Phone: +81-3-5802-3314, Fax: +81-3-5802-3315, mkano-tky@m.u-tokyo.ac.jp.

Kano and Hashimoto, 2009; Katz and Shatz, 1996; Lichtman and Colman, 2000; Purves and Lichtman, 1980; Watanabe and Kano, 2011). Postnatal refinement of climbing fiber (CF) to Purkinje cell (PC) synapses in the cerebellum has been a representative model of synapse elimination in the developing brain (Crepel, 1982; Hashimoto and Kano, 2005; Lohof et al., 1996; Watanabe and Kano, 2011). At birth, multiple CFs with similar synaptic strengths innervate the soma of each PC. A single CF is selectively strengthened among multiple CFs in each PC during the first postnatal week, and then only the strengthened CF (the "winner" CF) extends its innervation over dendrites of each PC. In contrast, surplus weaker CFs (the "loser" CFs) are left on the PC soma and then mostly eliminated during the second postnatal week (Bosman et al., 2008; Hashimoto et al., 2009a; Hashimoto and Kano, 2003, 2005; Watanabe and Kano, 2011). One-to-one connection from CF to PC dendrites is established in most PCs by the end of the third postnatal week (Watanabe and Kano, 2011). Several molecules responsible for mediating neural activity are involved in CF synapse elimination, including the type 1 metabotropic glutamate receptor (mGluR1) (Ichise et al., 2000; Kano et al., 1997), P/Q-type voltage-dependent Ca^{2+} channel (VDCC) (Hashimoto et al., 2011; Miyazaki et al., 2004), NMDA-type glutamate receptor (Kakizawa et al., 2000; Rabacchi et al., 1992) and glutamic acid decarboxylase 1 (Nakayama et al., 2012). Importantly, decreasing PC activity in mice by either overexpression of chloride channels or PC-selective deletion of P/Q-type VDCC impairs CF synapse elimination (Hashimoto et al., 2011; Lorenzetto et al., 2009). However, it remains unclear how PC activity determines CF synapse elimination.

Arc (also known as *Arg3.1*) is a well-known immediate early gene that acts as an effector protein downstream of multiple neuronal signaling pathways (Bramham et al., 2008; Shepherd and Bear, 2011). The function of Arc has been characterized in the hippocampus and cerebral cortex as having a role in synaptic plasticity (Guzowski et al., 2000; Okuno et al., 2012; Plath et al., 2006), homeostatic plasticity (Shepherd et al., 2006; Turrigiano, 2008) and experience-dependent plasticity in the remodeling of neocortical circuits (McCurry et al., 2010; Wang et al., 2006). Recently, Arc has been shown to function as "inverse tags" of inactive synapses and specifically accumulate at weaker synapses to prevent their undesired enhancement (Okuno et al., 2012). Although Arc was reported to be required for the late-phase of long-term depression (LTD) in cultured cerebellar PCs (Smith-Hicks et al., 2010), the roles Arc plays in developmental synapse elimination have not been addressed.

To explore the possible involvement of Arc in activity-dependent CF synapse elimination, we used *in vitro* organotypic coculture preparations that consist of cerebellar slices and explants of the medulla oblongata containing the inferior olive, the origin of CFs (Uesaka et al., 2012). This olivo-cerebellar coculture well mimics *in vivo* cerebellar circuits and reproduces the processes of CF synapse formation and elimination with molecular mechanisms similar to those *in vivo* (Uesaka et al., 2012). Using this coculture preparation combined with optogenetics (Boyden et al., 2005) and lentivirus-mediated knockdown of genes of interest, we demonstrate that Arc is a critical postsynaptic mediator for activity-dependent CF synapse elimination downstream of P/Q-type VDCC in PCs. Furthermore, our study in the developing cerebellum *in vivo* confirmed the results and further revealed that Arc is specifically involved in eliminating surplus CF synapses on the PC soma at the final stage of CF synapse elimination.

RESULTS

Two-Day Excitation of PCs Accelerates CF Synapse Elimination

To elucidate how PC activity mediates CF synapse elimination, we first examined the effect of increasing PC activity on CF synapse elimination using the coculture preparations. PCs at 10–12 days *in vitro* (DIV) exhibited spontaneous firing at 17.0 ± 2.5 Hz (Figure S1A, n =

10), which is comparable to the spontaneous firing rate of PCs in the rodent cerebellum *in vivo* during the second postnatal week (Woodward et al., 1969). This indicates that PCs in cocultures have similar level of activity to those in the developing cerebellum *in vivo*. To optically increase PC activity, we expressed channelrhodopsin-2 (ChR2)-EYFP in PCs under the control of PC-specific L7 promoter using a lentiviral gene transfer technique (Figure 1A) (Boyden et al., 2005; Sawada et al., 2010). We verified that blue light stimulation reliably evoked spiking in ChR2-expressing PCs under whole-cell current-clamp (Figure 1B) and cell-attached extracellular recording (Figure 1C) modes. Blue light pulses of 0.33 Hz faithfully evoked spiking in ChR2-expressing PCs (Figure 1B). To determine the light intensity for chronic photostimulation, we examined the efficacy of blue light stimulation to induce spikes in PCs with different light intensities. Maximal power density of a blue light emitting diode (LED, 470 nm) we used was 0.34 mW/mm^2 when measured 2 cm from the LED. Photostimulation of this power density increased the firing rate by 66.5 ± 8.8 Hz from the baseline activity in ChR2-expressing PCs (Figure 1D). This firing rate is approximately 4-fold higher than the spontaneous firing rate of PCs in the rodent cerebellum *in vivo* during the second postnatal week when CF synapse elimination occurs (Woodward et al., 1969). Therefore, we judged this stimulus strength to be sufficient for chronic photostimulation. While continuous 30-s photostimulation failed to drive spiking in the latter one third of illumination period, 1-s photostimulation reliably induced firing in PCs that persisted during stimulation (Figure 1B). Thus, we adopted 1 s of light exposure at 0.1 Hz for chronic photostimulation.

We applied 2-day photostimulation to cocultures from 10 or 11 DIV (Figure 1E), when redundant CFs are being eliminated (Uesaka et al., 2012). After the 2-day photostimulation, we examined CF innervation patterns in cocultures by using whole-cell recordings from ChR2-expressing and uninfected (control) PCs in the same slices. We found that 97% of photostimulated PCs were innervated by one or two CFs, while 58% of control PCs were innervated in the same way, indicating that CF synapse elimination was accelerated in photostimulated PCs (Figure 1E and 1F; $P = 0.0009$, Mann-Whitney U test). To exclude the possibility that either ChR2 expression or blue light illumination alone promoted CF synapse elimination, we compared (1) ChR2-expressing and uninfected (control) PCs in the absence of blue light (Figure S1B) and (2) EGFP-expressing and uninfected (control) PCs with the 2-day blue light illumination (Figure S1D). In both (1) and (2), there was no significant difference in CF innervation between infected and uninfected control PCs (Figure S1B–S1E; (1): $P = 0.2232$, (2): $P = 0.1596$, Mann-Whitney U test). These results demonstrate that chronically increasing PC activity promotes CF synapse elimination. Other electrophysiological parameters of CF-PC synapses and membrane properties of PCs were similar between photostimulated and control PCs (see Supplemental Text and Table S1). Moreover, the formation and function of parallel fiber (PF)-PC synapses were normal in photostimulated PCs (see Supplemental Text and Figures S1F and S1G).

P/Q-Type VDCC Mediates the Acceleration of CF Synapse Elimination

P/Q-type VDCC is a major high-threshold VDCC in PCs and has been demonstrated to mediate CF synapse elimination in the developing cerebellum (Hashimoto et al., 2011; Miyazaki et al., 2004). We hypothesized that the acceleration of CF synapse elimination by ChR2-mediated elevation of PC activity was caused by the increase of Ca^{2+} influx through P/Q-type VDCC. To inhibit the function of P/Q-type VDCC in PCs, we constructed lentiviruses containing engineered microRNA (miRNA) targeting P/Q-type VDCC (P/Q miRNA) and a fluorescent protein under the control of L7 promoter (see Supplemental Text and Figure S2A–S2C). Using this construct, we confirmed that P/Q-type VDCC was required for CF synapse elimination in cocultures as well as *in vivo* (Hashimoto et al., 2011; Miyazaki et al., 2004) (see Supplemental Text and Figure S2D and S2E).

We examined whether P/Q-type VDCC plays a role in the acceleration of CF synapse elimination by the 2-day photostimulation. There was no significant difference in the amplitude of inward currents evoked by 1-s blue light stimulation between PCs with ChR2 expression + P/Q miRNA expression (P/Q knockdown) and those with ChR2 expression alone (Figure S2F and S2G; $P = 0.4450$, Mann-Whitney U test), indicating similar expression level of ChR2. We applied the 2-day blue light illumination to three groups of coculture, namely cocultures containing PCs with ChR2 expression (yellow), those with ChR2 expression + P/Q knockdown (red) and those with EGFP expression + P/Q knockdown (green), from 10 or 11 DIV, when the majority of PCs are innervated by 4 or more CFs (Uesaka et al., 2012). Uninfected (control) PCs sampled from the three groups of coculture exhibited similar CF innervation patterns (Figure 2C; $P = 0.8505$, Kruskal-Wallis test), which enabled us to compare CF innervation patterns within the three groups of infected PCs. We found that the CF innervation patterns within the three groups significantly differed from each other (Figure 2B; $P < 0.0001$, Kruskal-Wallis test). We found that a significantly higher number of CFs innervated PCs with ChR2 expression + P/Q knockdown (red) when compared to those with ChR2 expression alone (yellow) (Figure 2B; $P = 0.0412$, Steel-Dwass test). This observation demonstrates that the acceleration of CF synapse elimination by the 2-day excitation of PCs is significantly attenuated by P/Q knockdown. Thus, Ca^{2+} influx through P/Q-type VDCC is an important factor for the acceleration of CF synapse elimination. On the other hand, a significantly higher number of CFs innervated PCs with EGFP expression + P/Q knockdown (green) when compared to those with ChR2 expression + P/Q knockdown (red) (Figure 2B; $P = 0.0461$, Steel-Dwass test), suggesting that residual P/Q-type VDCCs after knockdown, and/or other voltage-dependent mechanisms, might contribute to the acceleration of CF synapse elimination.

P/Q-Type VDCC Mediates Activity-Dependent Expression of Arc in PCs

Neural activity induces a number of Ca^{2+}-dependent genes that are involved in synapse development, maturation and refinement (Greer and Greenberg, 2008). Previous studies demonstrate that CF synapse elimination is an activity-dependent process mediated by P/Q-type VDCC (Hashimoto and Kano, 2005; Hashimoto et al., 2011; Miyazaki et al., 2004). Thus, we considered the possibility that some Ca^{2+}-dependent genes regulate CF synapse elimination in the cerebellum. We focused on an immediate early gene, *Arc*, because its expression is tightly coupled to neural activity downstream of multiple signaling pathways (Bramham et al., 2008; Shepherd and Bear, 2011) including Ca^{2+} influx through VDCC (Adams et al., 2009). Arc mRNA is detectable in PCs in the mouse cerebellum at an early postnatal stage, and its expression increases during postnatal development (Allen Brain Atlas; http://mouse.brain-map.org). We confirmed this expression pattern by comparing Arc mRNA expression level in the mouse cerebellum at postnatal day 9 (P9) and P16 by real-time PCR. Arc mRNA expression level at P16 was higher than 2-fold than that at P9, indicating that the expression of Arc significantly increases during the period of CF synapse elimination (Figure 3A; left, normalized by HPRT, $P = 0.0005$; right, normalized by GAPDH, $P = 0.0159$, Student's t test).

To examine whether Arc expression in PCs is activity-dependent, we used *Arc-pro-Venus-pest* transgenic mice in which a Venus fluorescent reporter is expressed under the control of Arc promoter (Kawashima et al., 2009). We made cocultures of cerebellar slices derived from *Arc-pro-Venus-pest* transgenic mice and explants of medulla oblongata. Robust expression of Arc was observed mainly in PCs by either membrane depolarization (high K^+, 60 mM) (Figure 3B) or optogenetic excitation (1-s blue light exposure at 0.1 Hz) (Figure S3A). The increase of Arc expression was suppressed when ω-agatoxin IVA (0.4 μM) was applied in the high K^+-containing culture medium (Figure 3B). Similar suppression of high K^+-induced elevation of Arc expression was observed in cocultures with PC-specific P/Q

knockdown (Figure S3B). We further confirmed the activity-dependent expression of endogenous Arc in PCs by immunohistochemistry using anti-Arc antibody (Figure 3C). These results indicate that Arc is expressed in PCs in an activity-dependent manner, which requires the activation of P/Q-type VDCC in PCs.

Since neural activity along PFs is considered to activate mGluR1 in PCs and to drive CF synapse elimination (Ichise et al., 2000; Kakizawa et al., 2000; Kano et al., 1997), we tested whether activation of mGluR1 in cocultures could elevate Arc expression in PCs. We applied an mGluR1 agonist, RS-3, 5-dihydroxyphenylglycine (DHPG, 100 μM), to cocultures from *Arc-pro-Venus-pest* transgenic mice and found that DHPG failed to elevate Arc expression (Figure S3C). We also found that the high K^+-induced increase of Arc expression was not suppressed by an mGluR1 antagonist, LY367385 (100 μM) (Figure S3C). These results indicate that mGluR1 itself is not essential for inducing Arc expression in PCs.

Arc Mediates CF Synapse Elimination in Cocultures

To examine whether Arc is involved in CF synapse elimination, we constructed lentiviruses expressing engineered miRNA directed against Arc (Arc miRNA) together with EGFP under L7 promoter. Introduction of Arc miRNA robustly reduced Arc expression to background (only-GFP-expressing) level in Arc-overexpressed HEK293T cells (Figure S4A and S4B; $P < 0.0001$, Dunnett test). Arc miRNA also reduced the activity-dependent expression of Arc in PCs in cocultures (Figure S4C).

We found that 66% of PCs expressing Arc miRNA (Arc knockdown PCs) were innervated by three or more CFs whereas 23% of uninfected (control) PCs were innervated in the same way at 15–17 DIV (Figure 4A and 4B). The frequency distribution histograms clearly show that Arc knockdown PCs were innervated by a significantly higher number of CFs than control PCs (Figure 4B, $P = 0.0003$, Mann-Whitney U test). The 10–90% rise time of CF-mediated excitatory postsynaptic currents (CF-EPSCs) was similar between Arc knockdown PCs and control PCs, while the total amplitude of CF-EPSCs was significantly larger in Arc knockdown PCs than in control PCs (Table S1; $P = 0.0094$, Mann-Whitney U test). We then checked whether selective strengthening of a single CF among multiple CFs was influenced by Arc knockdown. We calculated the disparity ratio and disparity index for each multiply innervated PCs, which have been used for estimating relative strengths of CF inputs (see Supplemental Experimental Procedures) (Hashimoto and Kano, 2003). We found that both parameters were similar between Arc knockdown PCs and control PCs (Table S1). These results indicate that Arc mediates CF synapse elimination in cocultures. We verified the specificity of the effect of Arc knockdown on CF synapse elimination by demonstrating that Arc miRNA-2, another non-overlapping miRNA construct directed against Arc, impaired CF synapse elimination in the same way as Arc miRNA (see Supplemental Text and Figure S4A–S4E).

Arc Is Required for the Acceleration of CF Synapse Elimination

P/Q-type VDCC mediates the acceleration of CF synapse elimination caused by elevation of PC activity (Figure 2). Arc is expressed in PCs in an activity-dependent manner, which requires the activation of P/Q-type VDCC in PCs (Figures 3 and S3). Therefore, it is legitimate to assume that Arc may be necessary for the acceleration of CF synapse elimination. To test this possibility, we examined the effect of Arc knockdown on its acceleration. We combined ChR2 expression and Arc knockdown by coexpressing Arc miRNA and ChR2-EYFP in PCs of cocultures by using lentiviruses. We applied the 2-day blue light illumination to three groups of coculture, namely cocultures containing PCs with ChR2 expression (yellow), those with ChR2 expression + Arc knockdown (red) and those

with EGFP expression + Arc knockdown (green), from 10 or 11 DIV (Figure 5A). Uninfected (control) PCs sampled from the three groups of coculture exhibited similar CF innervation patterns (Figure 5C; $P = 0.4702$, Kruskal-Wallis test). In contrast, there was a significant difference in the CF innervation patterns within the three groups of infected PCs (Figure 5B; $P < 0.0001$, Kruskal-Wallis test). We found that a significantly higher number of CFs innervated PCs with ChR2 expression + Arc knockdown (red) when compared to those with ChR2 expression alone (yellow) (Figure 5B; $P = 0.0283$, Steel-Dwass test). This finding demonstrates that Arc knockdown inhibits the acceleration of CF synapse elimination by the 2-day excitation of PCs. Together with the observations that Arc is tightly coupled with PC activity (Figures 3 andS3), these results suggest that activity-dependent expression of Arc is a key step to the acceleration of CF synapse elimination. On the other hand, a significantly higher number of CFs innervated PCs with EGFP expression + Arc knockdown (green) when compared to those with ChR2 expression + Arc knockdown (red) (Figure 5B; $P = 0.0412$, Steel-Dwass test), suggesting that residual Arc molecules after knockdown, and/or other activity-dependent mechanisms, might contribute to the acceleration of CF synapse elimination.

Arc Mediates CF Synapse Elimination in Vivo

To examine the role of Arc in CF synapse elimination *in vivo*, we injected lentiviruses expressing Arc miRNA together with EGFP under the control of L7 promoter into the mouse cerebellar vermis at P2–3 (Iizuka et al., 2009). The cerebella were examined at P19–26, when most PCs have become innervated by single CFs in wild-type mice. First we confirmed that EGFP was expressed predominantly in PCs in virus-injected mice (Figure 6A). Then we examined CF innervation patterns in virus-infected (Arc knockdown) and uninfected (control) PCs by using whole-cell recordings from PCs in acute cerebellar slices. We found that PCs with Arc knockdown were innervated by a significantly higher number of CFs than control PCs (Figure 6B and 6C; $P = 0.0002$, Mann-Whitney U test), indicating that the regression of surplus CFs was impaired in Arc knockdown PCs. To exclude the possibility of off-target effect of Arc miRNA, we constructed lentiviruses that encode an Arc miRNA-resistant form of Arc (Arc-res) together with mOrange. Arc-res was shown to be refractory to Arc miRNA in HEK293T cells (Figure S5A and S5B). We injected the mixture of lentiviruses carrying Arc knockdown and Arc-res into the mouse cerebellum and found that most infected PCs exhibited expression of both EGFP (Arc knockdown) and mOrange (Arc-res). There was no significant difference in CF innervation patterns between PCs with Arc knockdown + Arc-res and uninfected (control) PCs (Figure 6E and 6F; $P = 0.8770$, Mann-Whitney U test). Thus, the impairment of CF synapse elimination in Arc knockdown PCs was rescued by exogenous expression of Arc-res in PCs. From these results, we conclude that Arc plays a pivotal role in CF synapse elimination *in vivo*.

We examined the effect of Arc knockdown on other parameters of CF-PC synaptic transmission. The total amplitude of CF-EPSCs was significantly larger in Arc knockdown PCs than in control PCs (Figure 6D; $P = 0.0008$, Mann-Whitney U test), which was compatible with the result of Arc knockdown in cocultures (Table S1). The larger amplitude of CF-EPSCs in Arc knockdown PCs was restored to the normal level when Arc-res was simultaneously expressed, indicating that the larger amplitude of EPSC was also attributable to Arc knockdown (Figure 6G; $P = 0.5056$, Mann-Whitney U test). The paired-pulse ratio of CF-EPSCs (Table S2; $P = 0.2568$, Mann-Whitney U test), disparity index and disparity ratio (Table S2; disparity index: $P = 0.1829$, disparity ratio: $P = 0.2100$, Mann-Whitney U test), and the 10–90% rise time of CF-EPSCs (Table S3) were similar between Arc knockdown PCs and control PCs. These results indicate that basic properties of CF-PC synapses and functional differentiation of CF inputs were not affected by Arc knockdown in PCs.

To further confirm the specificity of the effect of Arc knockdown on CF synapse elimination *in vivo*, we carried out additional experiments using Arc miRNA-2. We found that Arc miRNA-2 impaired CF synapse elimination and increased the total amplitude of CF-EPSCs exactly in the same way as Arc miRNA (see Supplemental Text and Figure S5C-S5J). Since Arc miRNA and Arc miRNA-2 had the same effects on CF synapse elimination, we used Arc miRNA in the following experiments.

We then examined whether Arc influences PF-PC synapses. The paired-pulse ratio of PF-mediated EPSCs (PF-EPSCs) was similar between Arc knockdown PCs and control PCs (Figure S5K and S5L; $P = 0.3030$, two-way ANOVA). The input-output curves of PF-EPSC amplitude relative to stimulation strength were not significantly different between Arc knockdown and control PCs (Figure S5K and S5M; $P = 0.3910$, two-way ANOVA). These observations suggest that the persistent innervation of multiple CFs observed in Arc knockdown PCs is not due to malformation or malfunction of PF-PC synapses.

Arc Is Involved in Elimination of CF Synapses on the PC Soma

Previous studies indicate that there are four distinct phases in postnatal development of CF-PC synapses (Hashimoto et al., 2009a; Kano and Hashimoto, 2009; Watanabe and Kano, 2011). Elimination of surplus CFs proceeds in two phases, the early phase from P7 to around P11 which is independent of PF-PC synapse formation and the late phase from around P12 to P17 which requires normal PF-PC synapse formation. Notably, CF synapses remaining on the PC soma are eliminated in the late phase and a mono innervation pattern is attained (Hashimoto et al., 2009a; Kano and Hashimoto, 2009; Watanabe and Kano, 2011). To examine whether loss of Arc influences the early phase of CF synapse elimination, we compared CF innervation patterns in Arc knockdown PCs and control PCs at P11–12. We found that there was no significant difference in CF innervation patterns between Arc knockdown PCs and control PCs, suggesting that the late phase rather than the early phase was affected by Arc knockdown (Figure 7A and 7B; $P = 0.5538$, Mann-Whitney U test). To examine whether Arc is involved in the removal of CF synapses around the PC soma, we quantified the number of somatic CF terminals in scrambled control Arc miRNA (Scr-Arc, control) and Arc knockdown mice at P20 by immunostaining of the CF terminal marker type 2 vesicular glutamate transporter (VGluT2). We verified that CF synapse elimination was not influenced by Scr-Arc expression (Figure S6A and S6B; $P = 0.8770$, Mann-Whitney U test). We found that 77% of Arc knockdown PCs had 3 or more VGluT2-labeled CF terminals around their somata, whereas only 11% of Scr-Arc PCs did so (Figure 7C–7E; $P < 0.0001$, Mann-Whitney U test), indicating that elimination of somatic CF synapses was impaired in Arc knockdown PCs. In contrast, the relative height of VGluT2-labeled CF terminals in the molecular layer was similar between Scr-Arc and Arc knockdown mice (Figure 7C, 7D and 7F; Scr-Arc, 70.4 ± 3.4%, 12 areas; Arc knockdown, 72.1 ± 2.7%, 12 areas; $P = 0.1124$, Mann-Whitney U test), indicating that extension of CFs along PC dendrites was not affected by Arc knockdown. Taken together, we conclude that Arc is involved in the removal of perisomatic CF synapses in the late phase of CF synapse elimination.

Arc Mediates CF Synapse Elimination Downstream of P/Q-Type VDCC

P/Q-type VDCC is crucial for inducing Arc expression in PCs (Figure 3 and S3). Since both P/Q-type VDCC and Arc are required for activity-dependent CF synapse elimination (Figures 2 and 5), Arc is considered to mediate CF synapse elimination downstream of P/Q-type VDCC. To check this possibility, we examined whether the effect of Arc knockdown on CF synapse elimination is occluded by, or is additive to, P/Q knockdown. We first verified that P/Q miRNA expressed in PCs *in vivo* at P2–3 completely eliminated the function of P/Q-type VDCC when examined at P9 by using two distinct constructs that

contained P/Q miRNA at the 5' side and the 3' side of a fluorescent protein (Figure S7A and S7B). We then injected the virus for P/Q knockdown together with that for Scr-Arc (P/Q knockdown + Scr-Arc) or with that for Arc knockdown (P/Q knockdown + Arc knockdown) into the mouse cerebellum at P2–3 (Figure 8A). We made acute cerebellar slices at P19–23 and examined CF innervation patterns of doubly infected PCs. We found that 47% of PCs with P/Q knockdown + Scr-Arc and 49% of PCs with P/Q knockdown + Arc knockdown were innervated by two or three CFs and there was no significant difference in CF innervation patterns between the two groups (Figure 8A and 8B; $P = 0.9417$, Mann-Whitney U test). About 80% of uninfected control PCs were innervated by single CFs in both groups, indicating that there was no experimental bias between the two groups (Figure S7C and S7D; $P = 0.7094$, Mann-Whitney U test). These results clearly demonstrate that the effect of Arc knockdown on CF synapse elimination was occluded by P/Q knockdown in PCs, and indicate that Arc mediates CF synapse elimination downstream of P/Q-type VDCC.

Finally, we tested whether Arc expression alone in PCs can promote CF synapse elimination without P/Q-type VDCC function. We examined the effect of Arc overexpression in P/Q knockdown PCs to determine whether exogenous expression of Arc rescues the impairment of CF synapse elimination caused by P/Q knockdown. We injected the virus for P/Q knockdown together with that for mOrange (P/Q knockdown + mOrange) or with that for Arc overexpression (P/Q knockdown + Arc overexpression) into the mouse cerebellum at P2–3 (Figure 8C). We found that 51% of PCs with P/Q knockdown + mOrange and 43% of PCs with P/Q knockdown + Arc overexpression were innervated by two or three CFs at P20–23 and there was no significant difference in CF innervation patterns between the two groups (Figure 8C and 8D; $P = 0.4702$, Mann-Whitney U test). Again, about 80% of uninfected control PCs were innervated by single CFs in both groups, indicating that there was no significant experimental bias between the two groups (Figure S7C and S7D; $P = 0.9229$, Mann-Whitney U test). These results demonstrate that Arc overexpression alone cannot rescue the impaired CF synapse elimination in P/Q knockdown PCs. Thus, whereas Arc activation is essential, Arc may cooperate with other factors induced by P/Q-type VDCC-mediated Ca^{2+} elevation in PCs to collectively accomplish the late phase of CF synapse elimination.

DISCUSSION

Previous studies in the neuromuscular junction (Favero et al., 2009; Thompson, 1983) and the cerebellum (Lorenzetto et al., 2009) have indicated that postsynaptic activity is crucial for synapse elimination. However, the mechanisms as to how postsynaptic activity mediates synapse elimination and which activity-dependent mediators are involved have remained unclear. In this study, we showed that Arc expression increased in the developing cerebellum during the period of CF synapse elimination and its activity-dependent expression in PCs required P/Q-type VDCC. Then, we demonstrated that Arc knockdown in PCs suppressed the enhancement of CF synapse elimination by increasing PC activity in olivo-cerebellar coculture preparations *in vitro*. Finally, we found that Arc knockdown in PCs in the developing cerebellum *in vivo* resulted in a significant impairment of CF synapse elimination. These results indicate that Arc is a critical postsynaptic mediator for activity-dependent CF synapse elimination downstream of P/Q-type VDCC.

Our previous studies indicate that P/Q-type VDCC mediates most of the Ca^{2+} transients into PCs during CF activity (Hashimoto et al., 2011) and that P/Q-type VDCC in PCs is required for selective strengthening of a single "winner" CF in each PC, dendritic translocation of the "winner" CF, and elimination of weak "loser" CF synapses from the PC soma (Hashimoto et al., 2011; Miyazaki et al., 2004). In the present study, we found that PC-specific Arc knockdown *in vivo* did not affect the disparity index and disparity ratio, the height of CF

synaptic terminals in the molecular layer, and CF innervation patterns at P11–12. These results indicate that the selective strengthening of a single CF in each PC, the dendritic translocation of the strengthened CF, and the early phase of CF synapse elimination are not affected by PC-specific Arc knockdown. While these three phases of CF synapse elimination are severely impaired in PC-selective P/Q-type VDCC knockout mice (Hashimoto et al., 2011), Arc does not seem to be a downstream mediator of P/Q-type VDCC for these events during the first 10 days of postnatal cerebellar development.

Since endogenous Arc mRNA expression exhibits more than 2-fold increase from P9 to P16, Arc is considered to play an important role in the late phase of CF synapse elimination. We found that Arc knockdown in PCs *in vivo* at P2–3 did not affect CF innervation when examined at P11–12, but significantly impaired CF synapse elimination thereafter, particularly in the removal of redundant CF synapses from PC somata. The effect of Arc knockdown on CF synapse elimination was completely occluded by simultaneous P/Q knockdown, indicating that Arc mediates CF synapse elimination downstream of P/Q-type VDCC. In contrast, Arc overexpression in PCs did not rescue the impaired CF synapse elimination caused by P/Q knockdown. Therefore, Arc is considered to require other factors induced by P/Q-type VDCC-mediated Ca^{2+} elevation in PCs to remove redundant CF synapses from PC somata during the late phase of CF elimination. Previous studies have clarified that mGluR1 to protein kinase Cγ (PKCγ) cascade in PCs is crucial for the late phase of CF synapse elimination (Ichise et al., 2000; Kano et al., 1995; Kano et al., 1997; Kano et al., 1998; Offermanns et al., 1997). Besides this pathway involving mGluR1, the present study demonstrates that P/Q-type VDCC-mediated Ca^{2+} elevation and Arc activation is another activity-dependent pathway for the late phase of CF synapse elimination. It remains to be investigated whether and how these two pathways interact in PCs to eliminate redundant CF synapses on the PC soma.

It has been demonstrated that both long-term potentiation (LTP) and LTD occur at CF-PC synapses in rats (Bosman et al., 2008) and mice (Ohtsuki and Hirano, 2008) during the first postnatal week. Importantly, LTP has been reported to occur exclusively at strong CF inputs that can produce spikes and significant Ca^{2+} transients, whereas LTD has been shown to be induced at weak CF inputs that are not associated with Ca^{2+} transients (Bosman et al., 2008). The LTP and LTD during the first postnatal week may contribute to selective strengthening of single CF inputs and the prevention of other CF inputs from potentiation in individual PCs (Bosman et al., 2008; Ohtsuki and Hirano, 2008). These processes are not considered to involve Arc. In contrast, only LTD has been reported at CF-PC synapses during the second and third postnatal weeks (Hansel and Linden, 2000) when Arc seems to contribute to CF synapse elimination. Since the loss of Arc is reported to impair LTD in hippocampal neurons (Plath et al., 2006) and cultured cerebellar PCs (Smith-Hicks et al., 2010), it is possible that Arc may also be involved in the expression of LTD at CF-PC synapses. Moreover, previous studies in the hippocampus indicate that Arc plays an important role in the trafficking of AMPA-type glutamate receptors (AMPARs) (Chowdhury et al., 2006; Shepherd et al., 2006; Turrigiano, 2008). Our observation that the amplitude of CF-EPSC in Arc knockdown PCs was larger than control PCs suggests that Arc may be involved in AMPAR endocytosis in PCs, which leads to LTD of CF-EPSCs. It is therefore possible that Arc-mediated AMPAR endocytosis and the resultant LTD at CF-PC synapses may contribute to the weakening and eventual elimination of redundant CF synapses. A similar mechanism can be seen in the developing neuromuscular junction, where the decrease of postsynaptic acetylcholine receptors precedes the withdrawal of the overlying presynaptic terminals during synapse elimination (Colman et al., 1997).

Disordered expression of Arc has recently been reported in neurodevelopmental diseases including Fragile X syndrome and tuberous sclerosis (Auerbach et al., 2011; Park et al.,

2008). Furthermore, Arc is also shown to be a direct target of the ubiquitin ligase Ube3a (Greer et al., 2010). *Ube3a* is a disease gene in Angelman syndrome, a neurodevelopmental disorder characterized by various dysfunctions including cerebellar ataxia (Jiang et al., 1998). Since the present study demonstrates essential roles of Arc in synapse elimination in the developing cerebellum, it is possible that some symptoms of Arc disorder might be related to abnormality of neural circuit organization and function. Therefore, it is important to examine whether and how Arc contributes to neural circuit formation and refinement in brain regions that are considered to be relevant to the symptoms.

EXPERIMENTAL PROCEDURES

Animals

Sprague-Dawley (SD) rats and C57BL/6 mice were used (SLC JAPAN). All experiments were performed according to the guidelines laid down by the animal welfare committees of the University of Tokyo and the Japan Neuroscience Society. Lines of transgenic mice harboring the *Arc-pro-Venus-pest* transgene were generated in C57BL/6 by a method similar to that used for establishing *Arc-pro-EGFP-Arc* transgenic mice (Okuno et al., 2012). Detailed characterization of *Arc-pro-Venus-pest* transgenic mice will be described elsewhere (H.O. and H.B., in preparation). Other details are described in Supplemental Experimental Procedures.

Olivocerebellar Cocultures and Photostimulation

The olivo-cerebellar cocultures were prepared as described previously (Uesaka et al., 2012). In brief, the ventral medial portion of the medulla containing inferior olivary neurons was dissected from rat embryo at embryonic day 15, and cocultures with a cerebellar slices of 250 μm thickness from P10 mice. For continuous photostimulation of cocultures in a humidified incubator, a blue LED was placed onto each culture dish with a distance of the LED and the coculture of 2 cm. Other details are described in Supplemental Experimental Procedures.

Viral Vector Constructs

VSV-G pseudotyped lentiviral vectors (pCL20c) (Hanawa et al., 2002) were designed for PC-specific expression under the control of a truncated L7 promoter (pCL20c-L7) (Sawada et al., 2010). For vector-based RNAi analysis, we used BLOCK-iT Pol II miR RNAi expression vector kit (Invitrogen). The engineered miRNA constructs were produced by PCR amplification of miRNA region in BLOCK-iT Pol II miR RNAi expression vector followed by subcloning into pCL20c-L7 at 5’- or 3’-side of a fluorescent protein or ChR2 as indicated in the figures. Other details for preparation of viral vector constructs and methods for virus infection are described in Supplemental Experimental Procedures.

Electrophysiology

Recordings from PCs in the cocultures are performed as described previously (Uesaka et al., 2012) and are detailed in Supplemental Experimental Procedures. To stimulate CFs, square voltage pulses (duration, 0.1 ms; amplitude, 0–90 V) were applied between two of the eight tungsten electrodes placed in the medullary explants. All possible combinations of two electrodes were tested, and stimulus intensity was carefully increased from 0 V to 90 V for each stimulation pair so as not to miss the CFs innervating the recorded PC.

Preparation of acute cerebellar slices and recording from PCs are made as described previously (Hashimoto and Kano, 2003; Hashimoto et al., 2009b) and are detailed in Supplemental Experimental Procedures. To record CF-EPSCs, stimuli (duration, 0.1 ms; amplitude, 0–90 V) were applied at 0.2 Hz through a patch pipette filled with normal

external solution. CFs were stimulated in the granule cell layer 20–100 μm away from the PC soma. For each PC, the pipette for CF stimulation was moved systematically by about 20 μm step around the PC soma and the stimulus intensity was increased gradually from 0 V to about 90 V at each stimulation site. The number of CFs innervating the recorded PC was estimated by the number of discrete CF-EPSC steps as previously described (Hashimoto and Kano, 2003; Hashimoto et al., 2009b).

Statistical Analysis

All statistical values were presented as mean ± SEM unless indicated otherwise. Mann-Whitney U test or Student's t test was used as indicated in the text when two independent samples were compared. For multiple comparison, Kruskal-Wallis test, Steel-Dwass test, Dunnett test and two-way ANOVA were used as indicated in the text. Statistical analysis was conducted with JMP Pro. Differences between data sets were judged to be significant at $P < 0.05$. *, **, *** and **** represents $P < 0.05$, $P < 0.01$, $P < 0.001$ and $P < 0.0001$, respectively.

Supplementary Material

Refer to Web version on PubMed Central for supplementary material.

Acknowledgments

The authors thank A. Nienhuis, St. Jude Children's Research Hospital and George Washington University for the gifts of the lentiviral backbone vector and the packaging plasmid; T. Nakazawa for helpful advice for real-time PCR; K. Kitamura and K. Hashimoto for helpful discussions; M. Mahoney for critically reading this manuscript; and K. Matsuyama, M. Sekiguchi, S. Tanaka and A. Koseki for technical assistance. This work was supported by Grants-in-Aid for Scientific Research (17023021, 21220006 and 23650204 to M.K.; 21500301 and 24300117 to H.O.; 20670002 to H.B.), the Strategic Research Program for Brain Sciences (Development of biomarker candidates for social behavior) and the Global COE Program (Integrative Life Science Based on the Study of Biosignaling Mechanisms) from MEXT, Japan., by Grant-in Aid from MHLW, Japan (to H.O. and H.B.), and by CREST grant from JST, Japan (to H.B.).

REFERENCES

Adams JP, Robinson RA, Hudgins ED, Wissink EM, Dudek SM. NMDA receptor-independent control of transcription factors and gene expression. Neuroreport. 2009; 20:1429–1433. [PubMed: 19794318]

Arsenault D, Zhang ZW. Developmental remodelling of the lemniscal synapse in the ventral basal thalamus of the mouse. J. Physiol. 2006; 573:121–132. [PubMed: 16581865]

Auerbach BD, Osterweil EK, Bear MF. Mutations causing syndromic autism define an axis of synaptic pathophysiology. Nature. 2011; 480:63–68. [PubMed: 22113615]

Bosman LW, Takechi H, Hartmann J, Eilers J, Konnerth A. Homosynaptic long-term synaptic potentiation of the "winner" climbing fiber synapse in developing Purkinje cells. J. Neurosci. 2008; 28:798–807. [PubMed: 18216188]

Boyden ES, Zhang F, Bamberg E, Nagel G, Deisseroth K. Millisecond-timescale, genetically targeted optical control of neural activity. Nat. Neurosci. 2005; 8:1263–1268. [PubMed: 16116447]

Bramham CR, Worley PF, Moore MJ, Guzowski JF. The immediate early gene Arc/Arg3.1: regulation, mechanisms, and function. J. Neurosci. 2008; 28:11760–11767. [PubMed: 19005037]

Buffelli M, Burgess RW, Feng G, Lobe CG, Lichtman JW, Sanes JR. Genetic evidence that relative synaptic efficacy biases the outcome of synaptic competition. Nature. 2003; 424:430–434. [PubMed: 12879071]

Chen C, Regehr WG. Developmental remodeling of the retinogeniculate synapse. Neuron. 2000; 28:955–966. [PubMed: 11163279]

Chowdhury S, Shepherd JD, Okuno H, Lyford G, Petralia RS, Plath N, Kuhl D, Huganir RL, Worley PF. Arc/Arg3.1 interacts with the endocytic machinery to regulate AMPA receptor trafficking. Neuron. 2006; 52:445–459. [PubMed: 17088211]

Colman H, Nabekura J, Lichtman JW. Alterations in synaptic strength preceding axon withdrawal. Science. 1997; 275:356–361. [PubMed: 8994026]

Crepel F. Regression of functional synapses in the immature mammalian cerebellum. Trends. Neurosci. 1982; 5:266–269.

Favero M, Massella O, Cangiano A, Buffelli M. On the mechanism of action of muscle fibre activity in synapse competition and elimination at the mammalian neuromuscular junction. Eur. J. Neurosci. 2009; 29:2327–2334. [PubMed: 19490025]

Greer PL, Greenberg ME. From synapse to nucleus: calcium-dependent gene transcription in the control of synapse development and function. Neuron. 2008; 59:846–860. [PubMed: 18817726]

Greer PL, Hanayama R, Bloodgood BL, Mardinly AR, Lipton DM, Flavell SW, Kim TK, Griffith EC, Waldon Z, Maehr R, et al. The Angelman Syndrome protein Ube3A regulates synapse development by ubiquitinating Arc. Cell. 2010; 140:704–716. [PubMed: 20211139]

Guzowski JF, Lyford GL, Stevenson GD, Houston FP, McGaugh JL, Worley PF, Barnes CA. Inhibition of activity-dependent Arc protein expression in the rat hippocampus impairs the maintenance of long-term potentiation and the consolidation of long-term memory. J. Neurosci. 2000; 20:3993–4001. [PubMed: 10818134]

Hanawa H, Kelly PF, Nathwani AC, Persons DA, Vandergriff JA, Hargrove P, Vanin EF, Nienhuis AW. Comparison of various envelope proteins for their ability to pseudotype lentiviral vectors and transduce primitive hematopoietic cells from human blood. Mol. Ther. 2002; 5:242–251. [PubMed: 11863413]

Hansel C, Linden DJ. Long-term depression of the cerebellar climbing fiber-Purkinje neuron synapse. Neuron. 2000; 26:473–482. [PubMed: 10839365]

Hashimoto K, Ichikawa R, Kitamura K, Watanabe M, Kano M. Translocation of a “winner” climbing fiber to the Purkinje cell dendrite and subsequent elimination of “losers” from the soma in developing cerebellum. Neuron. 2009a; 63:106–118. [PubMed: 19607796]

Hashimoto K, Kano M. Functional differentiation of multiple climbing fiber inputs during synapse elimination in the developing cerebellum. Neuron. 2003; 38:785–796. [PubMed: 12797962]

Hashimoto K, Kano M. Postnatal development and synapse elimination of climbing fiber to Purkinje cell projection in the cerebellum. Neurosci. Res. 2005; 53:221–228. [PubMed: 16139911]

Hashimoto K, Tsujita M, Miyazaki T, Kitamura K, Yamazaki M, Shin HS, Watanabe M, Sakimura K, Kano M. Postsynaptic P/Q-type Ca^{2+} channel in Purkinje cell mediates synaptic competition and elimination in developing cerebellum. Proc. Natl. Acad. Sci. USA. 2011; 108:9987–9992. [PubMed: 21628556]

Hashimoto K, Yoshida T, Sakimura K, Mishina M, Watanabe M, Kano M. Influence of parallel fiber-Purkinje cell synapse formation on postnatal development of climbing fiber-Purkinje cell synapses in the cerebellum. Neuroscience. 2009b; 162:601–611. [PubMed: 19166909]

Hensch TK. Critical period regulation. Annu. Rev. Neurosci. 2004; 27:549–579. [PubMed: 15217343]

Ichise T, Kano M, Hashimoto K, Yanagihara D, Nakao K, Shigemoto R, Katsuki M, Aiba A. mGluR1 in cerebellar Purkinje cells essential for long-term depression, synapse elimination, and motor coordination. Science. 2000; 288:1832–1835. [PubMed: 10846166]

Iizuka A, Takayama K, Torashima T, Yamasaki M, Koyama C, Mitsumura K, Watanabe M, Hirai H. Lentiviral vector-mediated rescue of motor behavior in spontaneously occurring hereditary ataxic mice. Neurobiol. Dis. 2009; 35:457–465. [PubMed: 19573599]

Jiang YH, Armstrong D, Albrecht U, Atkins CM, Noebels JL, Eichele G, Sweatt JD, Beaudet AL. Mutation of the Angelman ubiquitin ligase in mice causes increased cytoplasmic p53 and deficits of contextual learning and long-term potentiation. Neuron. 1998; 21:799–811. [PubMed: 9808466]

Kakizawa S, Yamasaki M, Watanabe M, Kano M. Critical period for activity-dependent synapse elimination in developing cerebellum. J. Neurosci. 2000; 20:4954–4961. [PubMed: 10864953]

Kano M, Hashimoto K. Synapse elimination in the central nervous system. Curr. Opin. Neurobiol. 2009; 19:154–161. [PubMed: 19481442]

Kano M, Hashimoto K, Chen C, Abeliovich A, Aiba A, Kurihara H, Watanabe M, Inoue Y, Tonegawa S. Impaired synapse elimination during cerebellar development in PKC γ mutant mice. Cell. 1995; 83:1223–1231. [PubMed: 8548808]

Kano M, Hashimoto K, Kurihara H, Watanabe M, Inoue Y, Aiba A, Tonegawa S. Persistent multiple climbing fiber innervation of cerebellar Purkinje cells in mice lacking mGluR1. Neuron. 1997; 18:71–79. [PubMed: 9010206]

Kano M, Hashimoto K, Watanabe M, Kurihara H, Offermanns S, Jiang H, Wu Y, Jun K, Shin HS, Inoue Y, et al. Phospholipase Cβ4 is specifically involved in climbing fiber synapse elimination in the developing cerebellum. Proc. Natl. Acad. Sci. USA. 1998; 95:15724–15729. [PubMed: 9861037]

Katz LC, Shatz CJ. Synaptic activity and the construction of cortical circuits. Science. 1996; 274:1133–1138. [PubMed: 8895456]

Kawashima T, Okuno H, Nonaka M, Adachi-Morishima A, Kyo N, Okamura M, Takemoto-Kimura S, Worley PF, Bito H. Synaptic activity-responsive element in the Arc/Arg3.1 promoter essential for synapse-to-nucleus signaling in activated neurons. Proc. Natl. Acad. Sci. USA. 2009; 106:316–321. [PubMed: 19116276]

Konnerth A, Llano I, Armstrong CM. Synaptic currents in cerebellar Purkinje cells. Proc. Natl. Acad. Sci. USA. 1990; 87:2662–2665. [PubMed: 1969639]

Lichtman JW, Colman H. Synapse elimination and indelible memory. Neuron. 2000; 25:269–278. [PubMed: 10719884]

Lohof AM, Delhaye-Bouchaud N, Mariani J. Synapse elimination in the central nervous system: functional significance and cellular mechanisms. Rev. Neurosci. 1996; 7:85–101. [PubMed: 8819204]

Lorenzetto E, Caselli L, Feng G, Yuan W, Nerbonne JM, Sanes JR, Buffelli M. Genetic perturbation of postsynaptic activity regulates synapse elimination in developing cerebellum. Proc. Natl. Acad. Sci. USA. 2009; 106:16475–16480. [PubMed: 19805323]

Lu T, Trussell LO. Development and elimination of endbulb synapses in the chick cochlear nucleus. J. Neurosci. 2007; 27:808–817. [PubMed: 17251420]

McCurry CL, Shepherd JD, Tropea D, Wang KH, Bear MF, Sur M. Loss of Arc renders the visual cortex impervious to the effects of sensory experience or deprivation. Nat. Neurosci. 2010; 13:450–457. [PubMed: 20228806]

Miyazaki T, Hashimoto K, Shin HS, Kano M, Watanabe M. P/Q-type Ca^{2+} channel α1A regulates synaptic competition on developing cerebellar Purkinje cells. J. Neurosci. 2004; 24:1734–1743. [PubMed: 14973254]

Nakayama H, Miyazaki T, Kitamura K, Hashimoto K, Yanagawa Y, Obata K, Sakimura K, Watanabe M, Kano M. GABAergic inhibition regulates developmental synapse elimination in the cerebellum. Neuron. 2012; 74:384–396. [PubMed: 22542190]

Offermanns S, Hashimoto K, Watanabe M, Sun W, Kurihara H, Thompson RF, Inoue Y, Kano M, Simon MI. Impaired motor coordination and persistent multiple climbing fiber innervation of cerebellar Purkinje cells in mice lacking Gαq. Proc. Natl. Acad. Sci. USA. 1997; 94:14089–14094. [PubMed: 9391157]

Ohtsuki G, Hirano T. Bidirectional plasticity at developing climbing fiber-Purkinje neuron synapses. Eur. J. Neurosci. 2008; 28:2393–2400. [PubMed: 19032589]

Okuno H, Akashi K, Ishii Y, Yagishita-Kyo N, Suzuki K, Nonaka M, Kawashima T, Fujii H, Takemoto-Kimura S, Abe M, et al. Inverse synaptic tagging of inactive synapses via dynamic interaction of Arc/Arg3.1 with CaMKIIβ. Cell. 2012; 149:886–898. [PubMed: 22579289]

Park S, Park JM, Kim S, Kim JA, Shepherd JD, Smith-Hicks CL, Chowdhury S, Kaufmann W, Kuhl D, Ryazanov AG, et al. Elongation factor 2 and fragile X mental retardation protein control the dynamic translation of Arc/Arg3.1 essential for mGluR-LTD. Neuron. 2008; 59:70–83. [PubMed: 18614030]

Plath N, Ohana O, Dammermann B, Errington ML, Schmitz D, Gross C, Mao X, Engelsberg A, Mahlke C, Welzl H, et al. Arc/Arg3.1 is essential for the consolidation of synaptic plasticity and memories. Neuron. 2006; 52:437–444. [PubMed: 17088210]

Purves D, Lichtman JW. Elimination of synapses in the developing nervous system. Science. 1980; 210:153–157. [PubMed: 7414326]

Rabacchi S, Bailly Y, Delhaye-Bouchaud N, Mariani J. Involvement of the N-methyl D-aspartate (NMDA) receptor in synapse elimination during cerebellar development. Science. 1992; 256:1823–1825. [PubMed: 1352066]

Sawada Y, Kajiwara G, Iizuka A, Takayama K, Shuvaev AN, Koyama C, Hirai H. High transgene expression by lentiviral vectors causes maldevelopment of Purkinje cells *in vivo* . Cerebellum. 2010; 9:291–302. [PubMed: 20178014]

Shepherd JD, Bear MF. New views of Arc, a master regulator of synaptic plasticity. Nat. Neurosci. 2011; 14:279–284. [PubMed: 21278731]

Shepherd JD, Rumbaugh G, Wu J, Chowdhury S, Plath N, Kuhl D, Huganir RL, Worley PF. Arc/Arg3.1 mediates homeostatic synaptic scaling of AMPA receptors. Neuron. 2006; 52:475–484. [PubMed: 17088213]

Smith-Hicks C, Xiao B, Deng R, Ji Y, Zhao X, Shepherd JD, Posern G, Kuhl D, Huganir RL, Ginty DD, et al. SRF binding to SRE 6.9 in the Arc promoter is essential for LTD in cultured Purkinje cells. Nat. Neurosci. 2010; 13:1082–1089. [PubMed: 20694003]

Thompson W. Synapse elimination in neonatal rat muscle is sensitive to pattern of muscle use. Nature. 1983; 302:614–616. [PubMed: 6835395]

Turrigiano GG. The self-tuning neuron: synaptic scaling of excitatory synapses. Cell. 2008; 135:422–435. [PubMed: 18984155]

Uesaka N, Mikuni T, Hashimoto K, Hirai H, Sakimura K, Kano M. Organotypic coculture preparation for the study of developmental synapse elimination in mammalian brain. J. Neurosci. 2012; 32:11657–11670. [PubMed: 22915109]

Wang KH, Majewska A, Schummers J, Farley B, Hu C, Sur M, Tonegawa S. *In vivo* two-photon imaging reveals a role of Arc in enhancing orientation specificity in visual cortex. Cell. 2006; 126:389–402. [PubMed: 16873068]

Watanabe M, Kano M. Climbing fiber synapse elimination in cerebellar Purkinje cells. Eur. J. Neurosci. 2011; 34:1697–1710. [PubMed: 22103426]

Woodward DJ, Hoffer BJ, Lapham LW. Postnatal development of electrical and enzyme histochemical activity in Purkinje cells. Exp. Neurol. 1969; 23:120–139. [PubMed: 5765001]

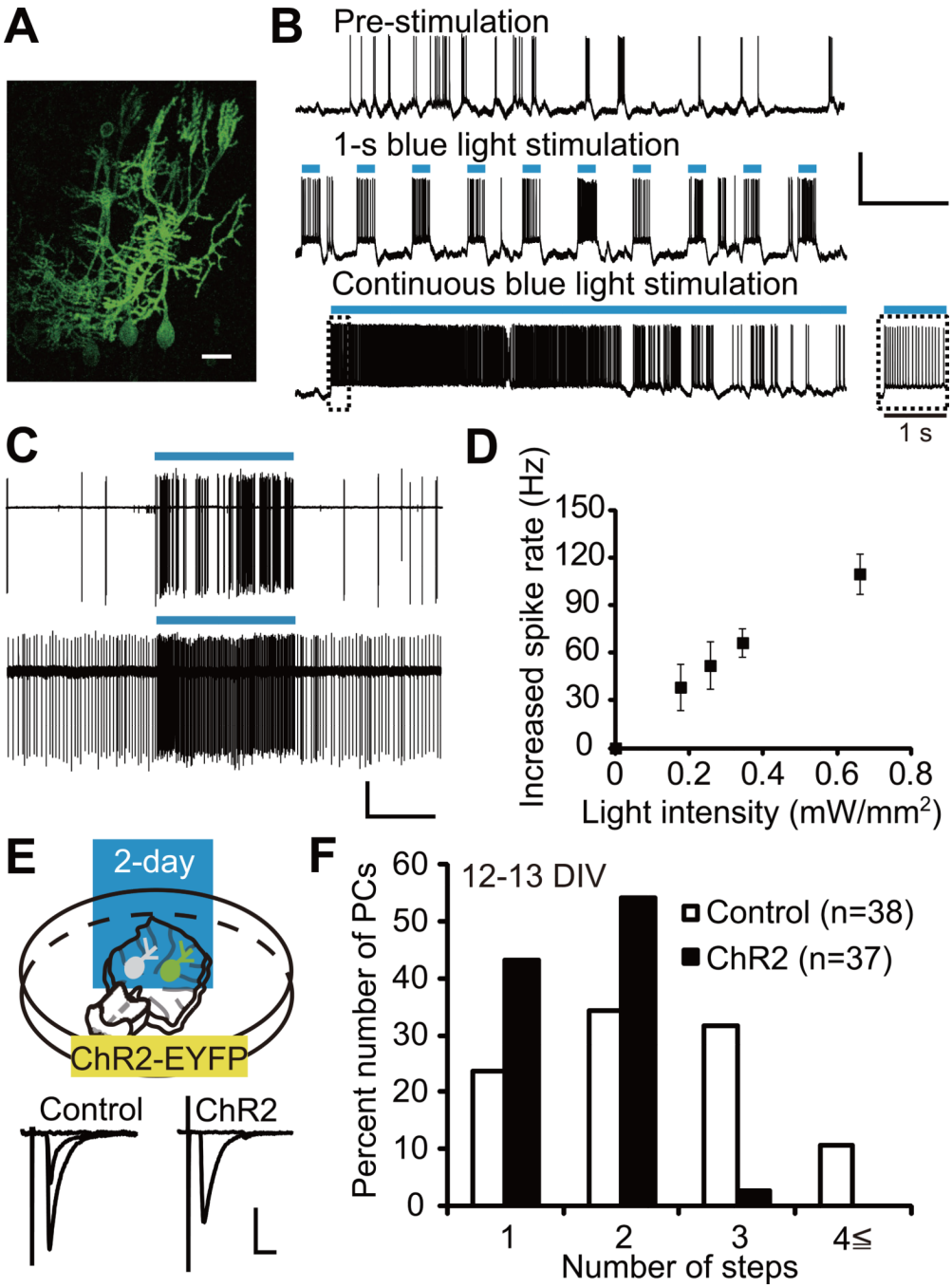

Figure 1. Two-Day Photostimulation of ChR2-Expressing PCs Accelerates CF Synapse Elimination

(A) PCs expressing ChR2-EYFP in an olivo-cerebellar coculture. Scale bar, 20 μm.

(B) Representative voltage traces under current-clamp mode from a PC expressing ChR2. Records were taken before photostimulation (top), during 1-s photostimulation at 0.33 Hz (middle) and during continuous photostimulation (bottom). Inset, expanded trace for the first 1 s of continuous photostimulation. Durations of photostimulation are indicated by blue bars. Scale bars, 5 s and 50 mV.

(C) Cell-attached recordings from two ChR2 expressing PCs. Scale bars, 5 s and 50 pA.

(D) Increase in firing rate against blue light intensity in PCs expressing ChR2-EYFP (n = 7 PCs from 4 cocultures). The number of spikes was counted during 1 s epoch before and during photostimulation.
(E) ChR2-EYFP was expressed in PCs and blue light stimulation (1-s light exposure at 0.1 Hz) was applied for two days from 10 or 11 DIV. Representative traces of CF-EPSC recorded from a control PC (left, “control” with 2 distinct EPSC steps) and a ChR2-expressing PC (right, “ChR2” with 1 EPSC step). Scale bars, 10 ms and 1 nA. Holding potential, −30 mV. Intensity for CF stimulation in the medullary explant was increased gradually and representative single traces recorded around individual threshold intensity were superimposed. Sample CF-EPSC traces in olivo-cerebellar cocultures are shown similarly in the following figures (Figures 2A, 4A and 5A).
(F) Frequency distribution histogram for the number of CFs innervating control (open columns, n = 38 PCs) and ChR2-expressing (filled columns, n = 37 PCs) PCs from 24 cocultures. The frequency distribution was significantly different between the two groups of PCs ($P = 0.0009$, Mann-Whitney U test).
See also Figure S1 and Table S1.

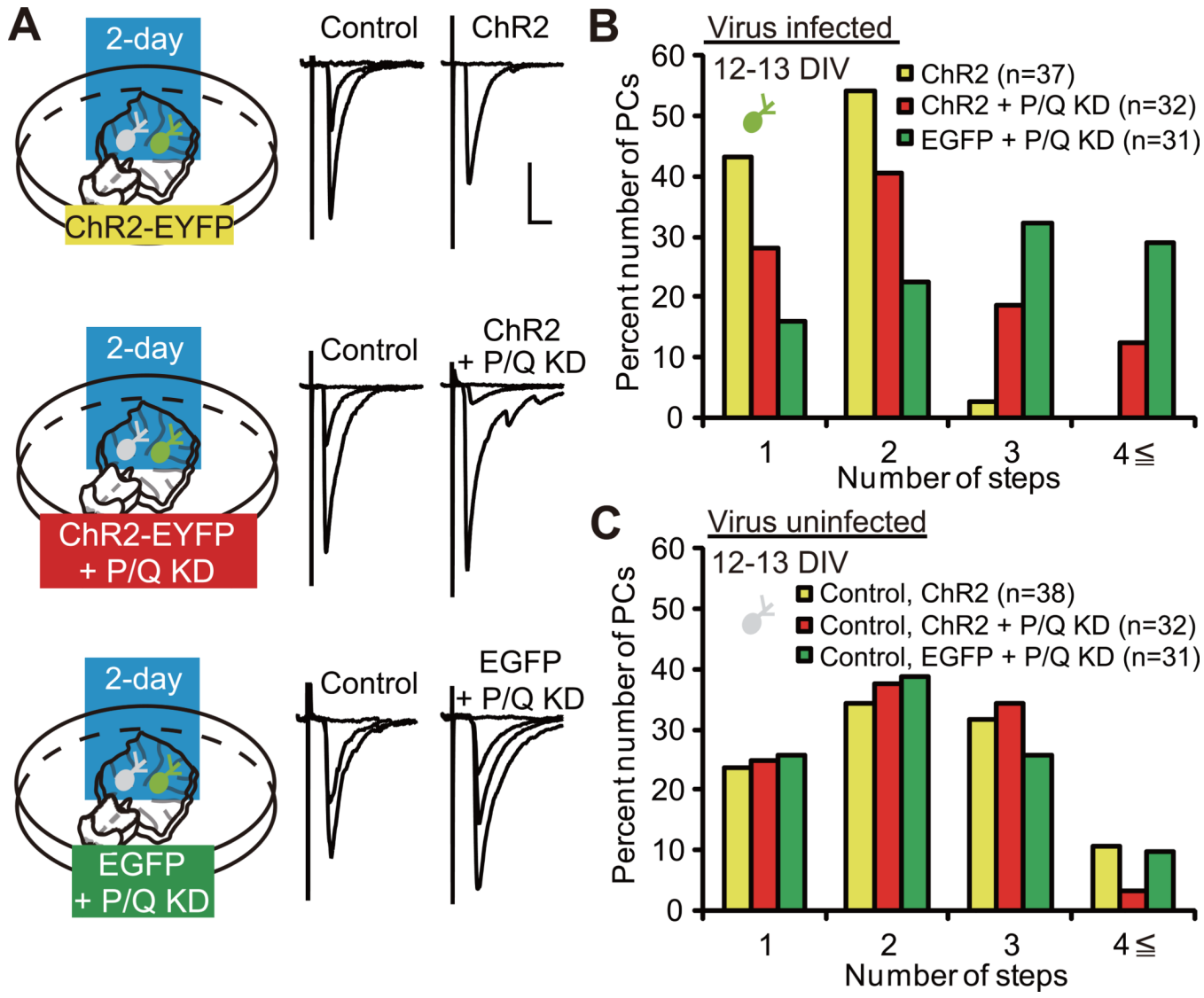

Figure 2. P/Q-Type VDCC Is Required for the Acceleration of CF Synapse Elimination

(A) PCs with ChR2 expression (top, “ChR2”), ChR2 expression + P/Q knockdown (KD) (middle, “ChR2 + P/Q KD”) and EGFP expression + P/Q KD (bottom, “EGFP + P/Q KD”) were illuminated with blue light for two days. Representative traces of CF-EPSCs recorded at 12–13 DIV. Scale bars, 10 ms and 1 nA. Holding potential, −30 mV.

(B) Frequency distribution histogram for the number of CFs innervating PCs with ChR2 (yellow columns, n = 37 PCs from 24 cocultures), ChR2 + P/Q KD (red columns, n = 32 PCs from 22 cocultures) and EGFP + P/Q KD (green columns, n = 31 PCs from 20 cocultures). A highly significant difference was noted in CF innervation patterns among the three groups of infected PCs ($P < 0.0001$, Kruskal-Wallis test). Frequency distribution was significantly different between PCs with ChR2 and those with ChR2 + P/Q KD ($P = 0.0412$, Steel-Dwass test) and PCs with ChR2 + P/Q KD and those with EGFP + P/Q KD ($P = 0.0461$, Steel-Dwass test).

(C) Frequency distribution histogram for the number of CFs innervating uninfected (control) PCs (yellow columns, control for ChR2, n = 38 PCs from 24 cocultures; red columns, control for ChR2 + P/Q KD, n = 32 PCs from 22 cocultures; and green columns, control for EGFP + P/Q KD, n = 31 PCs from 20 cocultures). There was no significant difference in

frequency distribution among the three groups of control PCs. $P = 0.8505$, Kruskal-Wallis test.

See also Figure S2.

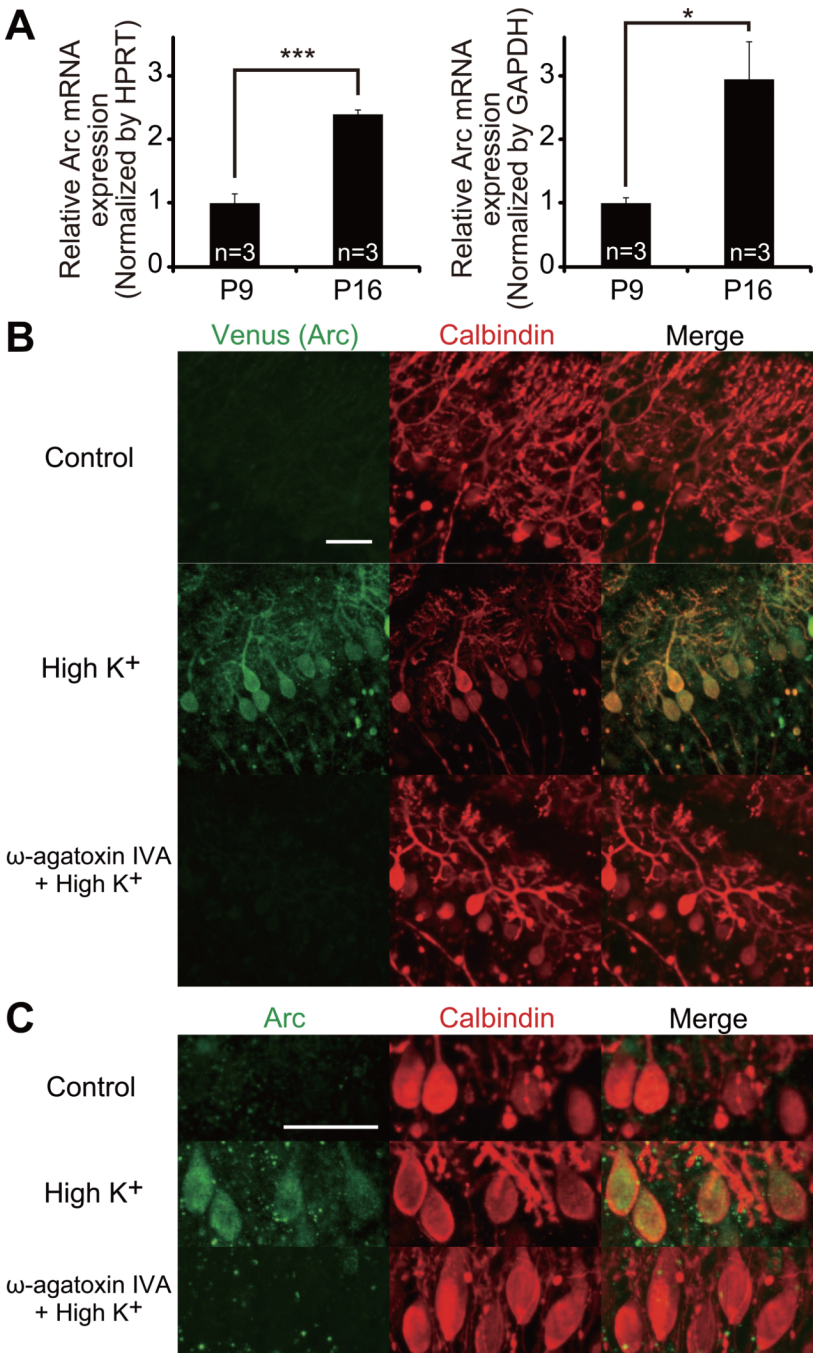

Figure 3. Developmental Increase of Arc Expression and Its Activity-Dependent Expression Mediated by P/Q-Type VDCC

(A) Quantification of Arc mRNA in the cerebellum at P9 and P16 by real-time PCR. The expression of Arc was normalized to that of internal standard hypoxanthine guanine phosphoribosyl transferase (HPRT, left) and glyceraldehydes-3-phosphate dehydrogenase (GAPDH, right), respectively (P9, 3 mice; P16, 3 mice). ***$P = 0.0005$, *$P = 0.0159$, Student's t test.

(B) Immunofluorescent labeling for Venus (Arc expression reporter, green) and calbindin (PCs, red) in cocultured cerebellar slices derived from *Arc-pro-Venus-pest* transgenic mice

at 13 DIV after 5 h incubation with control, high K^+ (60 mM) or ω-agatoxin IVA (0.4 μM) + high K^+-containing culture medium. Scale bar, 50 μm.

(C) Immunofluorescent labeling for Arc (green) and calbindin (red) in cocultured cerebellar slices derived from wild-type mice at 13 DIV after 5 h incubation with control, high K^+ or ω-agatoxin IVA + high K^+-containing culture medium. Scale bar, 50 μm.

See also Figure S3.

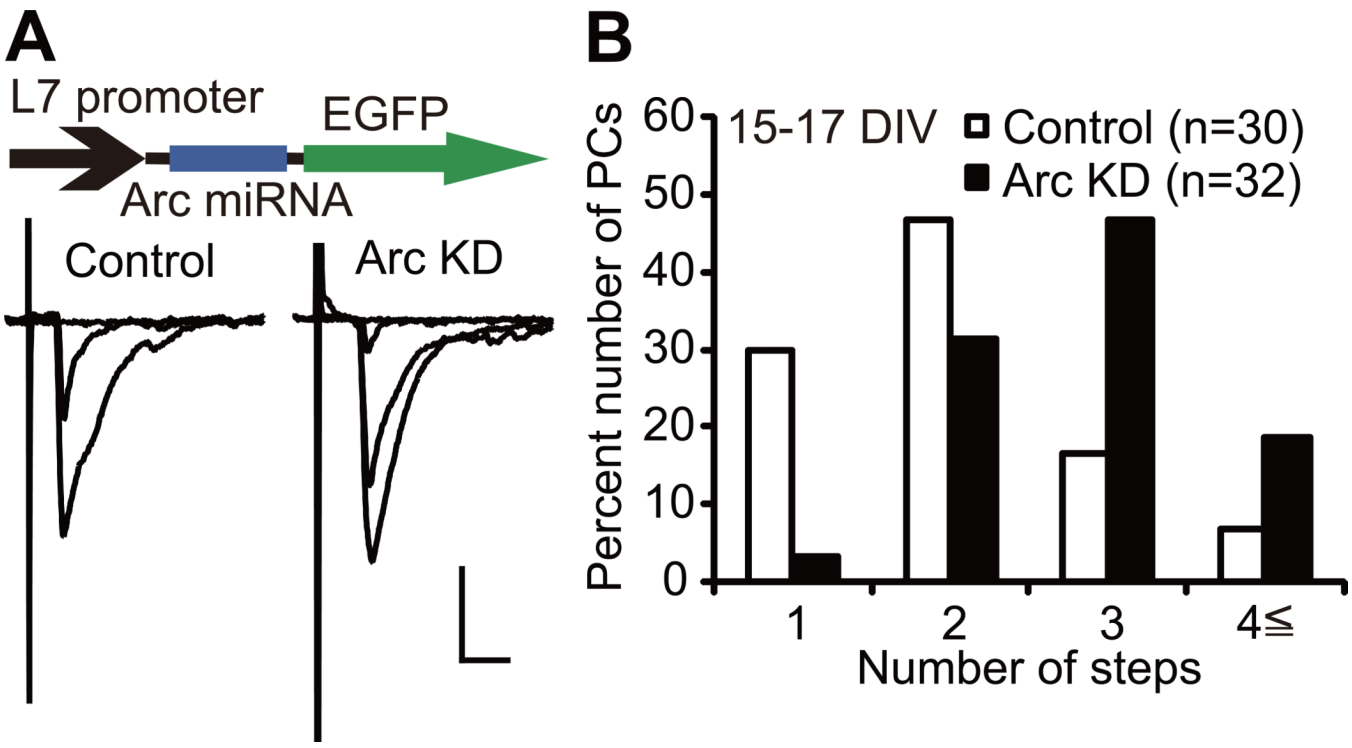

Figure 4. Arc Mediates CF Synapse Elimination in Cocultures

(A) Representative CF-EPSCs recorded at 15–17 DIV from a control uninfected PC (left) and a PC with Arc knockdown ("Arc KD", right). Scale bars, 10 ms and 1 nA. Holding potential, −30 mV.

(B) Frequency distribution histograms for the number of CFs innervating control PCs (open columns, n = 30 PCs) and PCs with Arc KD (filled columns, n = 32 PCs) from 21 cocultures. Frequency distributions are significantly different between the two groups of PCs (P = 0.0003, Mann-Whitney U test).

See also Figure S4 and Table S1.

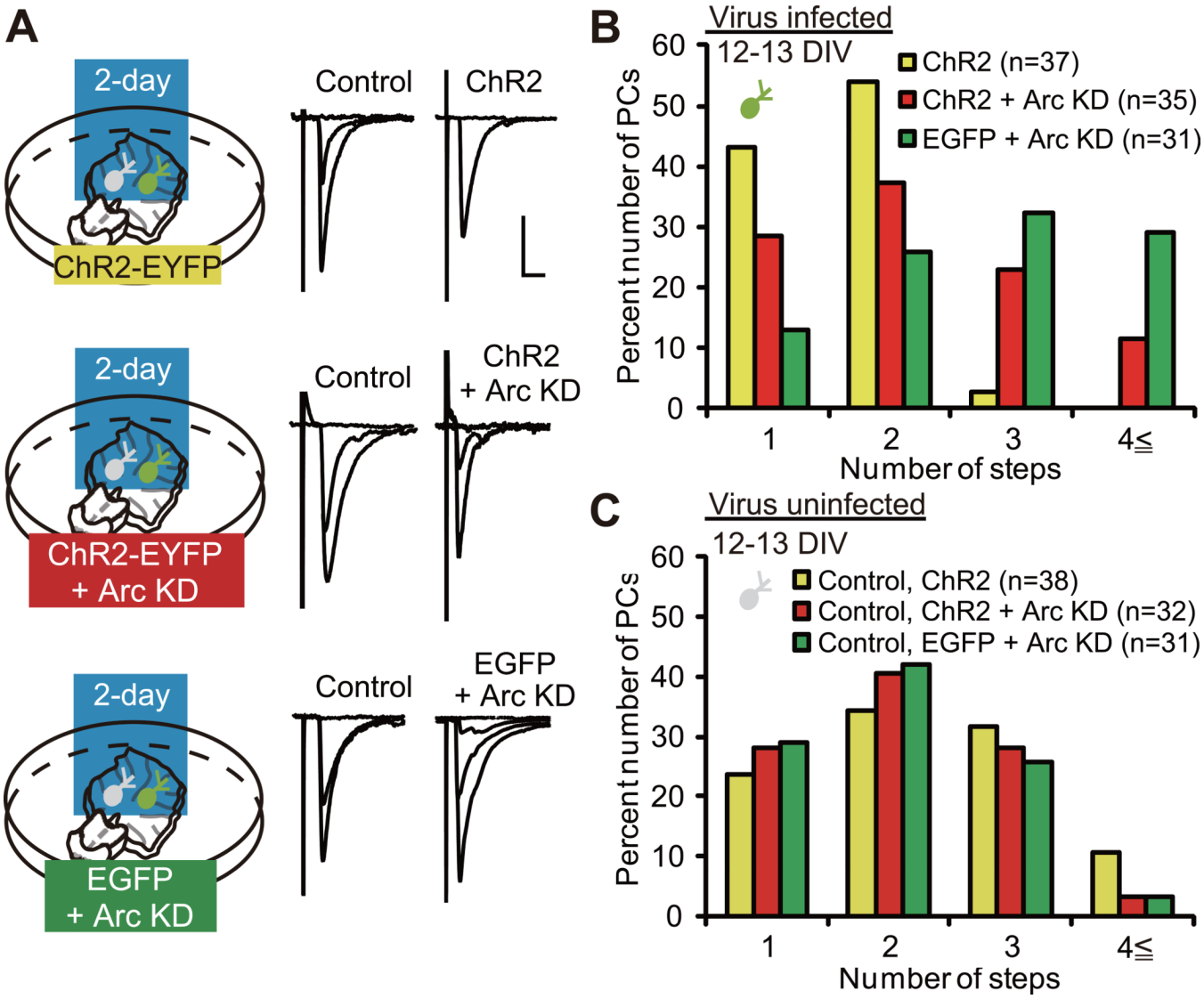

Figure 5. Arc Is Required for the Acceleration of CF Synapse Elimination

(A) PCs with ChR2 (top), ChR2 + Arc KD (middle) and EGFP + Arc KD (bottom) were illuminated with blue light for two days. Representative traces of CF-EPSCs recorded at 12–13 DIV. Scale bars, 10 ms and 1 nA. Holding potential, −30 mV.

(B) Frequency distribution histogram for the number of CFs innervating PCs with ChR2 (yellow columns, n = 37 PCs from 24 cocultures), ChR2 + Arc KD (red columns, n = 35 PCs from 23 cocultures) and EGFP + Arc KD (green columns, n = 31 PCs from 20 cocultures). A highly significant difference was noted in CF innervation patterns among the three groups of infected PCs ($P < 0.0001$, Kruskal-Wallis test). Frequency distribution was significantly different between PCs with ChR2 and those with ChR2 + Arc KD ($P = 0.0283$, Steel-Dwass test) and between PCs with ChR2 + Arc KD and those with EGFP + Arc KD ($P = 0.0412$, Steel-Dwass test).

(C) Frequency distribution histogram for the number of CFs innervating uninfected (control) PCs (yellow columns, control for ChR2, n = 38 PCs from 24 cocultures; red columns, control for ChR2 + Arc KD, n = 32 PCs from 23 cocultures; and green columns, control for EGFP + Arc KD, n = 31 PCs from 20 cocultures). There was no significant difference among the three groups of control PCs. $P = 0.4702$, Kruskal-Wallis test.

See also Figure S4.

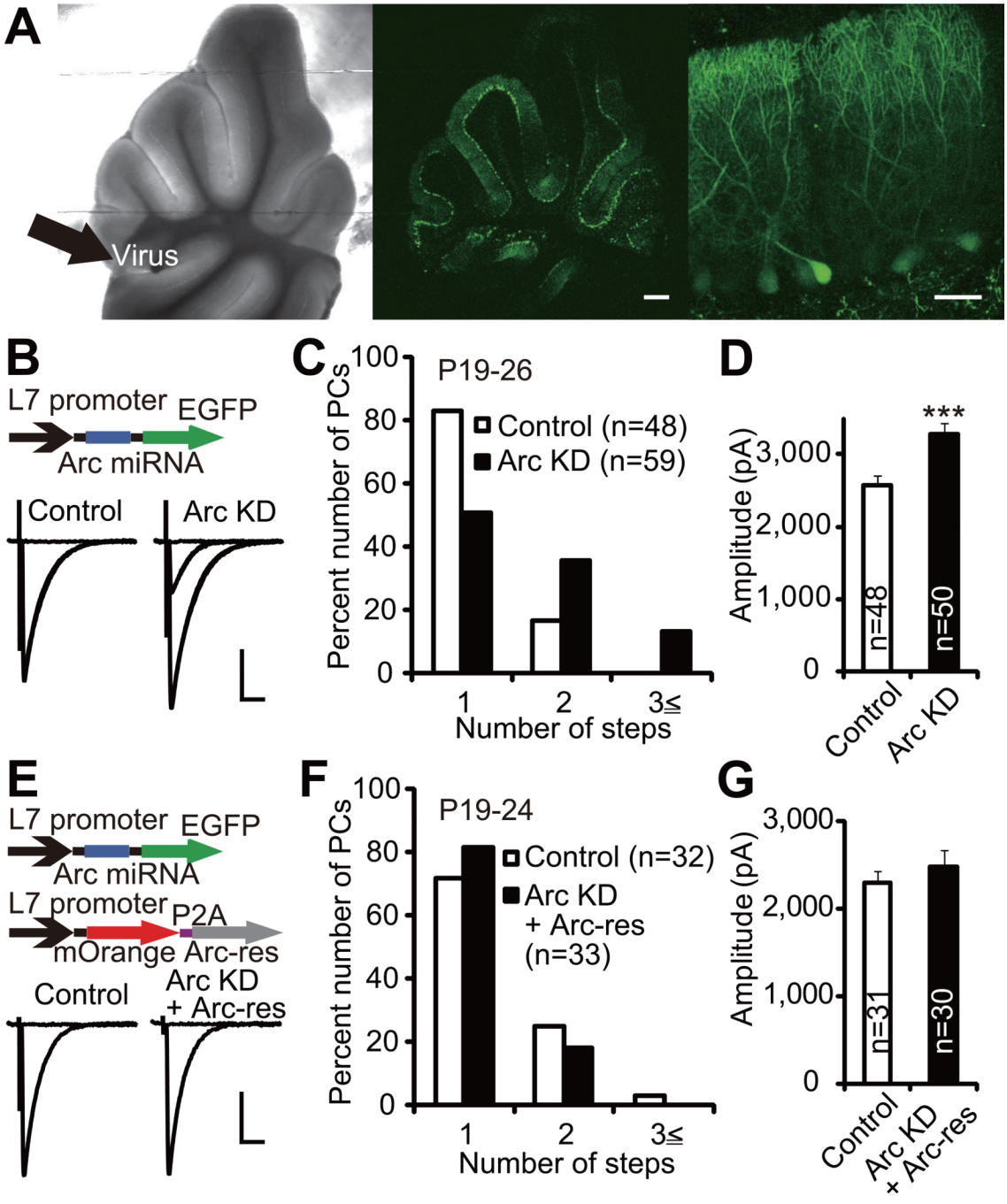

Figure 6. Arc Mediates CF Synapse Elimination In Vivo

(A) An acute slice from a lentivirus-injected cerebellum prepared at P20. Lentivirus encoding Arc miRNA and EGFP (Arc KD) was injected into the cerebellar vermis (left, indicated with thick arrow) at P2. Low (middle) and high (right) power focus of the same cerebellar slice for fluorescent signals showing PCs expressing EGFP. Scale bars, 0.5 mm (middle) and 50 μm (right).

(B) Representative traces of CF-EPSCs recorded from a control uninfected PC (left) and a PC with Arc KD (right). Lentivirus carrying Arc miRNA was injected into the cerebellar vermis at P2–3, and CF-EPSCs were recorded from PCs in acute cerebellar slices prepared from 10 mice at P19–26. For each PC, the pipette for CF stimulation was moved

systematically by about 20 μm step around the PC soma and the stimulus intensity was increased gradually at each stimulation site. For showing representative CF-EPSC traces, one to three CF-EPSC traces recorded around individual threshold intensity were superimposed. Sample CF-EPSC traces from acute cerebellar slices are shown similarly in the following figures (Figures 6E, 7A, 8A and 8C).

(C) Frequency distribution histograms for the number of CFs innervating control PCs (open columns, n = 48 PCs) and PCs with Arc KD (filled columns, n = 59 PCs). Frequency distributions are significantly different between the two groups of PCs ($P = 0.0002$, Mann-Whitney U test).

(D) Summary bar graphs for the total amplitude of CF-EPSCs in control PCs and PCs with Arc KD (control, n = 48 PCs; Arc KD, n = 50 PCs). ***$P = 0.0008$, Mann-Whitney U test.

(E) Representative traces of CF-EPSCs in an uninfected control PC (left) and a PC transfected with Arc KD + Arc miRNA-resistant form of Arc ("Arc-res", right). A mixture of lentiviral vectors carrying Arc KD and Arc-res was injected into the cerebellum at P2–3, and CF innervation patterns were examined in 7 mice at P19–24.

(F) Frequency distribution histogram for the number of CFs innervating control PCs (open columns, n = 32 PCs) and PCs transfected with Arc KD + Arc-res (filled columns, n = 33 PCs). No significant difference was detected between the two groups of PCs ($P = 0.8770$, Mann-Whitney U test).

(G) Summary bar graphs for the total amplitude of CF-EPSCs in control PCs and PCs transfected with Arc KD + Arc-res (control, n = 31 PCs; Arc KD + Arc-res, n = 30 PCs). No significant difference was detected between the two groups of PCs ($P = 0.5056$, Mann-Whitney U test).

Scale bars, 10 ms and 1 nA. Holding potential, −10 mV.

See also Figure S5 and Tables S2 and S3.

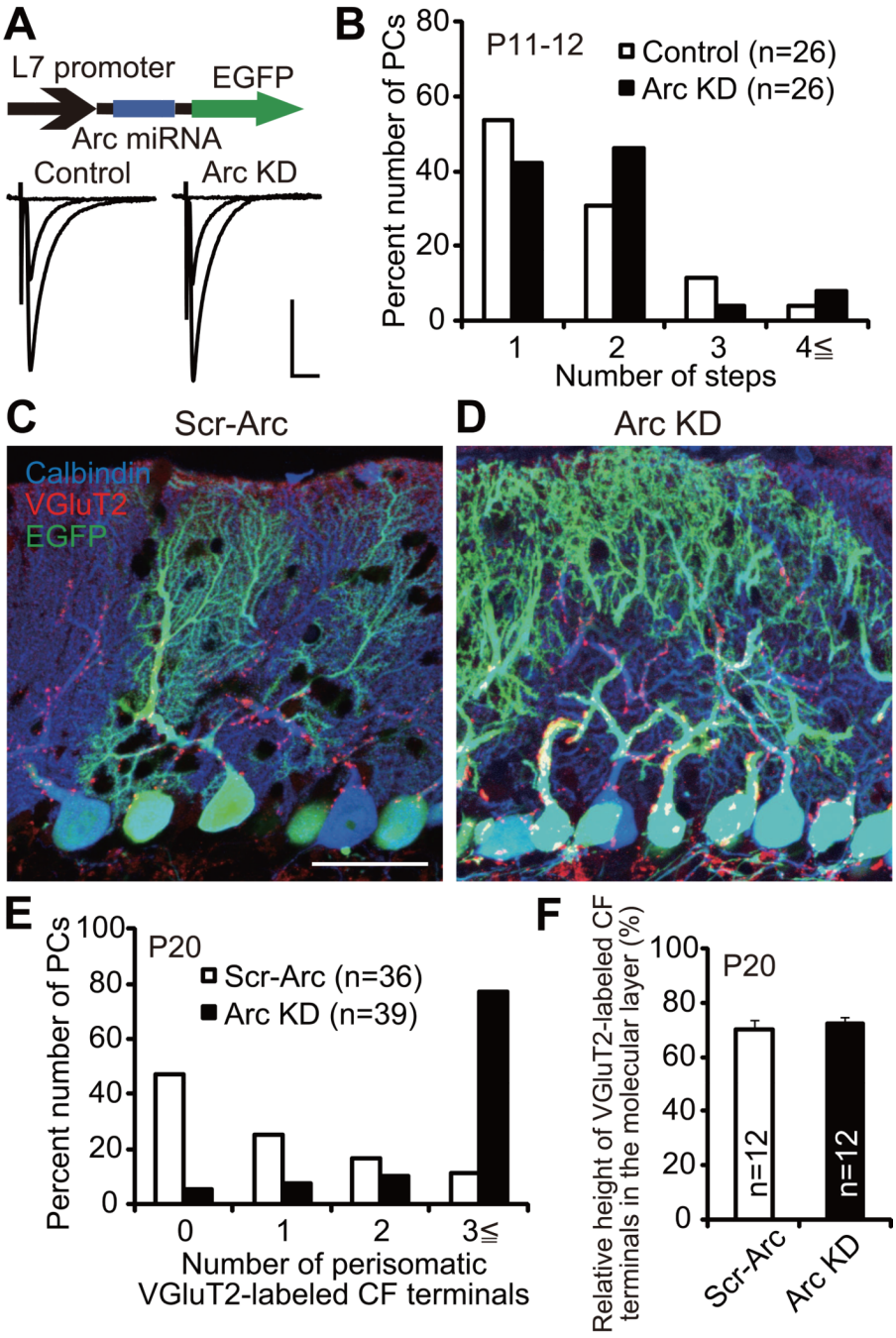

Figure 7. Persistent Perisomatic CF Innervations in Arc Knockdown PCs In Vivo

(A) Representative traces of CF-EPSCs from a control PC (left) and a PC with Arc KD (right). Lentivirus carrying Arc miRNA and EGFP was injected at P2–3, and CF-EPSCs were recorded at P11–12 from 5 mice. Scale bars, 10 ms and 1 nA. Holding potential, −10 mV.

(B) Frequency distribution histogram for the number of CFs innervating control PCs (open columns, n = 26 PCs) and PCs with Arc KD (filled columns, n = 26 PCs) at P11–12 from 5 mice. There was no significant difference between the two groups of PCs ($P = 0.5538$, Mann-Whitney U test).

(C and D) Confocal microscopic images of a cerebellum transfected with scrambled control Arc miRNA (“Scr-Arc”, C) and that with Arc KD (D) showing immunoreactivities for calbindin (blue, PCs), VGluT2 (red, CF terminals) and EGFP (green). Scale bar, 50 μm.
(E) Frequency distribution histogram for the number of perisomatic CF-terminals on PCs with Scr-Arc (open columns, n = 36 PCs from 2 mice) and those with Arc KD (filled columns, n = 39 PCs from 2 mice). A highly significant difference was noted between the two groups of PCs ($P < 0.0001$, Mann-Whitney U test).
(F) Relative height of VGluT2-labeled CF terminals in the molecular layer for Scr-Arc (open columns, n = 12 slices from 2 mice) and Arc KD (filled columns, n = 12 slices from 2 mice) cerebella. There was no significant difference between the two groups of PCs ($P = 0.1124$, Mann-Whitney U test).
See also Figure S6.

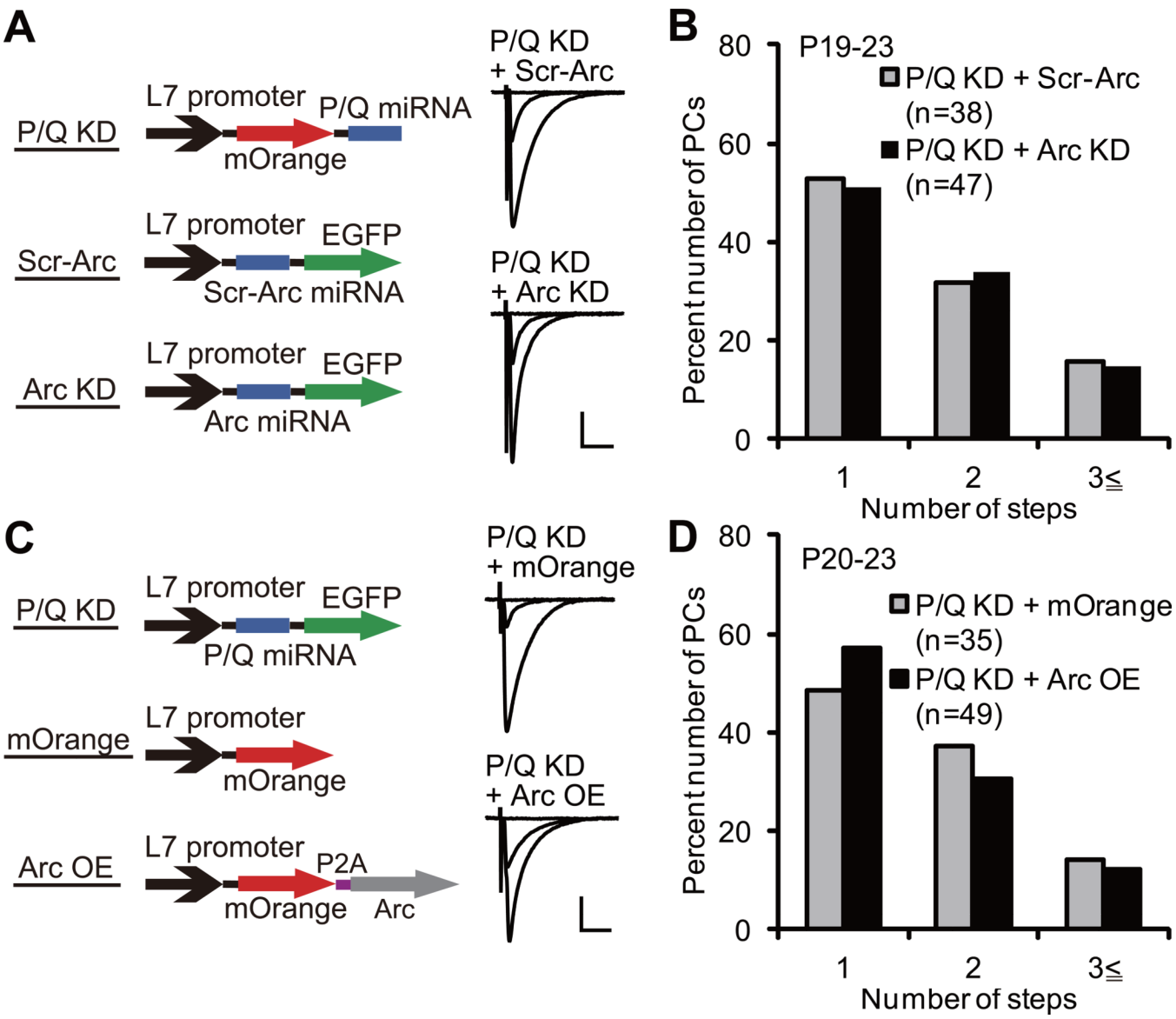

Figure 8. Arc Is a Necessary but Not Sufficient Mediator of CF Synapse Elimination Downstream of P/Q-Type VDCC

(A) Representative traces of CF-EPSCs from a PC with P/Q KD + Scr-Arc (upper) and that with P/Q KD + Arc KD (lower). A mixture of lentiviruses was injected at P2–3, and CF-EPSCs were recorded from 5 mice at P19–23 (P/Q KD + Scr-Arc) and 6 mice at P19–22 (P/Q KD + Arc KD).

(B) Frequency distribution histogram for the number of CFs innervating PCs with P/Q KD + Scr-Arc (gray columns, n = 38 PCs from 5 mice) and P/Q KD + Arc KD (filled columns, n = 47 PCs from 6 mice) showing no significant difference between the two groups of PCs (P = 0.9417, Mann-Whitney U test).

(C) Representative traces of CF-EPSCs from a PC with P/Q KD + lentivirus for mOrange expression (“mOrange”, upper) and that with P/Q KD + lentivirus for Arc overexpression (“Arc OE”, lower). A mixture of lentiviruses was injected at P2–3, and CF-EPSCs were recorded from 5 mice at P21–23 (P/Q KD + mOrange) and 7 mice at P20–23 (P/Q KD + Arc OE).

(D) Frequency distribution histogram for the number of CFs innervating PCs with P/Q KD + mOrange (gray columns, n = 35 PCs from 5 mice) and P/Q KD + Arc OE (filled columns, n = 49 PCs from 7 mice) showing no significant difference between the two groups of PCs (P = 0.4702, Mann-Whitney U test).
Scale bars, 10 ms and 1 nA. Holding potential, −10 mV.
See also Figure S7.